Petroleum Science 20 (2023) 309–321

Contents lists available at ScienceDirect

Petroleum Science

journal homepage: www.keaipublishing.com/en/journals/petroleum-science

Original Paper

# A semi-analytical rate-transient analysis model for light oil reservoirs exhibiting reservoir heterogeneity and multiphase flow

Jin-Chang Li [a, b], Bin Yuan [a, b, *], Christopher R. Clarkson [c], Jian-Quan Tian [a, b]

[a] Key Laboratory of Unconventional Oil & Gas Development (China University of Petroleum (East China)), Ministry of Education, Qingdao, 266580, Shandong, PR China
[b] School of Petroleum Engineering, China University of Petroleum (East China), Qingdao, 266580, Shandong, PR China
[c] Department of Geoscience, University of Calgary, AB, T2L2N5, Canada

ARTICLE INFO

*Article history:*
Received 8 June 2022
Received in revised form
16 September 2022
Accepted 20 September 2022
Available online 26 September 2022

Edited by Yan-Hua Sun

*Keywords:*
Transient linear flow
Multiphase flow
Reservoir heterogeneity
Unconventional reservoirs

ABSTRACT

Rate-transient analysis (RTA) has been widely applied to extract estimates of reservoir/hydraulic fracture properties. However, the majority of RTA techniques can lead to misdiagnosis of reservoir/fracture information when the reservoir exhibits reservoir heterogeneity and multiphase flow simultaneously. This work proposes a practical-yet-rigorous method to decouple the effects of reservoir heterogeneity and multiphase flow during TLF, and improve the evaluation of reservoir/fracture properties.

A new, general, semi-analytical model is proposed that explicitly accounts for multiphase flow, fractal-based reservoir heterogeneity, anomalous diffusion, and pressure-dependent fluid properties. This is achieved by introducing a new Boltzmann-type transformation, the exponent of which includes reservoir heterogeneity and anomalous diffusion. In order to decouple the effects of reservoir heterogeneity and multiphase flow during TLF, the modified Boltzmann variable allows the conversion of three partial differential equations (PDE's) (i.e., oil, gas and water diffusion equations) into ordinary differential equations (ODE's) that are easily solved using the Runge-Kutta (RK) method. A modified time-power-law plot is also proposed to estimate the reservoir and fracture properties, recognizing that the classical square-root-of-time-plot is no longer valid when various reservoir complexities are exhibited simultaneously. Using the slope of the straight line on the modified time-power-law plot, the linear flow parameter can be estimated with more confidence. Moreover, because of the new Boltzmann-type transformation, reservoir and fracture properties can be derived more efficiently without the need for defining complex pseudo-variable transformations.

Using the new semi-analytical model, the effects of multiphase flow, reservoir heterogeneity and anomalous diffusion on rate-decline behavior are evaluated. For the case of approximately constant flowing pressure, multiphase flow impacts initial oil rate, which is a function of oil relative permeability and well flowing pressure. However, multiphase flow has a minor effect on the oil production decline exponent. Reservoir heterogeneity/anomalous diffusion affect both the initial oil production rate and production decline exponent. The production decline exponent constant is a function of reservoir heterogeneity/anomalous diffusion only.

The practical significance of this work is the advancement of RTA techniques to allow for more complex reservoir scenarios, leading to more accurate production forecasting and better-informed capital planning.



## 1. Introduction

The rate-transient analysis (RTA) technique has been widely applied to estimate reservoir and fracture parameters (e.g., matrix reservoir permeability, fracture half-length, fluid-in-place, and etc.) in support of field development and optimization. For this purpose,

* Corresponding author. Key Laboratory of Unconventional Oil & Gas Development (China University of Petroleum (East China)), Ministry of Education, Qingdao, 266580, Shandong, PR China.
*E-mail address:* yuanbin@upc.edu.cn (B. Yuan).

https://doi.org/10.1016/j.petsci.2022.09.021

a variety of RTA models have been derived using analytical or semi-analytical solutions to the classical diffusion equations adopted to different flow regimes; however, these solutions require many simplifications to reservoir/well boundary conditions, fluid/rock properties, fracture geometry, etc. Despite these limitations, RTA models have been successfully applied to conventional reservoirs through application of superposition, pseudo-variables and rate-normalized pressure. The combination of these data conversion techniques allows for the application of single-phase liquid flow solutions for the constant rate case to be extended to reservoirs saturated with compressible fluids producing under variable flowing pressures/rates at the well.

However, the majority of RTA models fail to account for reservoir complexities commonly observed in unconventional tight/shale reservoirs, including multiphase flow, reservoir heterogeneity, pressure-dependent reservoir/fracture properties, and anomalous diffusion (AD) in heterogeneous reservoirs. As a consequence, significant errors can result from application of these RTA models to multi-fractured horizontal wells (MFHW) producing from unconventional reservoirs. Therefore, in the past two decades, significant effort has been made to extend the capabilities of RTA models so that they can be applied to more complex unconventional reservoirs.

For multiphase flow, several approaches have been used to derive analytical RTA model solutions, including the iterative integral method (Qanbari and Clarkson, 2013), the modified pseudo-variables method (Behmanesh et al., 2015; Yuan et al., 2015, 2017; Qanbari and Clarkson, 2016; Clarkson, 2021), and the similarity-based approach (Zhang et al., 2016; Hamdi et al., 2018). In addition, with more further simplifications (e.g., steady-state multiphase flow; one of multiphase is assumed approximately immobile), material-balance method (Shi et al., 2020; Li et al., 2021) have been applied to derive an analytical model. Among them, the most popular approach is to use modified pseudo-variables to linearize the multiphase flow equations; with this approach, saturation- and pressure-dependent fluid/reservoir properties are incorporated into the modified pseudo-variables (i.e., pseudo-pressure, pseudo-time), which is necessary to derive the solutions analytically (Behmanesh et al., 2015; Behmanesh, 2016; Yuan et al., 2017, 2021). A drawback of this approach, however, is that pseudo-variable calculation requires saturation–pressure relationships to be developed. For this purpose, Clarkson and Qanbari (2016) developed an empirical saturation–pressure relationship for oil/gas flow. Another alternative approach is to derive the saturation–pressure relationship by employing the Boltzmann variable to obtain the analytical or semi-analytical solutions (i.e., similarity-based solutions). The Boltzmann transformation allows the simplification of the governing partial differential equations (PDE's) to ordinary differential equations (ODE's). Boe et al. (1989) and Behmanesh et al. (2015) utilized the Boltzmann variable to derive the saturation–pressure relationship for two-phase flow for the constant-rate radial flow regime and constant-flowing-pressure linear flow regime, respectively. Zhang et al. (2016) proposed a modified similarity-based approach (using the Runge-Kutta method) for multiphase liquid-rich gas (LRG) reservoirs with two different inner-boundary conditions (i.e., constant-flowing-pressure and constant-rate) for two-phase linear and radial transient flow regimes. Hamdi et al. (2018) further developed a semi-analytical model using the similarity-based Runge-Kutta method to obtain saturation–pressure relationships as a function of the Boltzmann variable for three-phase flow in volatile oil reservoirs. Another key contribution of Hamdi et al. (2018) is that a straight-line analysis method was provided to derive the linear flow parameter without requiring pseudo-variables. Those authors later demonstrated practical applicability of the method to field data (Hamdi et al., 2020). However, all the available analytical models developed using the similarity-based method have only been applied to cases with uniform distributions of reservoir properties, and do not account for reservoir complexities such as reservoir heterogeneity.

For reservoir heterogeneity, Yuan et al. (2019a, b) developed analytical solutions for TLF by incorporating fractal-based matrix reservoir permeability gradients away from the primary fracture. Shahamat et al. (2018) modified the classical TLF solution (Wattenbarger et al., 1998) for the case of a non-uniform matrix reservoir permeability distribution. Acuña (2016) defined “fracture swarms” as “groups of near-parallel fractures with very small spacing” and generated a network of fractures with fractally distributed spacing; he demonstrated that this configuration (for high conductivity fractures) can cause sub-linear flow. In parallel with the above extensions of classical-diffusion-based solutions, researchers have developed analytical or semi-analytical anomalous-diffusion-based solutions incorporating matrix and fracture heterogeneity. Raghavan and Chen (2017, 2018) derived the analytical flowing solution for sub-linear flow caused by the combinations of fracture conductivity, fracture half-length, and fracture spacing for hydraulically fractured wells. Also, in the framework of anomalous diffusion (AD), the power-law decline model, based on analytical single-phase flow solutions in heterogeneous oil and gas reservoirs, has been applied by various researchers (Liu et al., 2018; Albinali and Ozkan, 2016; Wang et al., 2017; Holy and Ozkan, 2017; Al-Rebeawi, 2019; Artus et al., 2019; Valdes-Perez and Blasingame, 2020, etc.). However, all of the available anomalous-diffusion-based solutions are still limited by the assumption of single-phase flow of oil or gas, without consideration of multiphase flow. Yuan et al. (2021) derived a semi-analytical solution accounting for the combination of various reservoir complexities including anomalous diffusion, reservoir heterogeneity, multiphase flow, and pressure-dependent fluid and rock properties by using modified pseudo-variables. However, the practicality of this method is limited because the saturation–pressure relationship used for the calculation of pseudo-variables was derived from numerical reservoir simulation model output. In summary, to the best of our knowledge, an analytical RTA model, and associated saturation–pressure relationship, for the case of three-phase flow in heterogeneous reservoirs has not been developed. We believe that development of such a model is of practical importance to the analysis of many unconventional reservoirs.

The current work therefore proposes a new analytical RTA solution that explicitly accounts for multiphase flow, reservoir heterogeneity, anomalous diffusion, and pressure-dependent fluid properties. The fractal dimension and AD exponent are defined to account for non-uniform distribution of reservoir permeability and porosity. A new Boltzmann-type transformation, for which the exponent includes reservoir geometric heterogeneity and AD, is proposed for the first time. A theoretical explanation for the occurrence of non-straight-line behavior on the square-root-of-time plot for any of the producing phases (oil, water and gas) caused by reservoir heterogeneity and AD is provided. A modified time-power-law plot is also proposed to estimate reservoir and fracture properties. The new analytical model is verified by using a numerical reservoir simulation model and its practical application is demonstrated with a field case. Moreover, the individual effects of multiphase flow, reservoir heterogeneity and anomalous

diffusion on rate-decline behaviors in reservoirs exhibiting multiphase flow, reservoir heterogeneity and anomalous diffusion are investigated using the new analytical model.

## 2. Theory and methods

### 2.1. Mathematical model

In this section, a new, general, analytical model is proposed that explicitly accounts for multiphase flow, fractal-based reservoir heterogeneity and pressure-dependent fluid properties. Hydraulic fracturing is required to obtain the largest efficient production for unconventional reservoir. Yuan et al. (2019a) suggested that the quality of stimulated reservoir volume (SRV) is deteriorated caused by the limited energy of hydraulic fracturing. Following the work by Yuan et al. (2021), fractal theory is applied to characterize the geometric heterogeneity of reservoir permeability and porosity as follows:

$$\phi(x) = \phi_i \left(\frac{x}{x_i}\right)^{D-1} \tag{1}$$

$$k(x) = k_i \left(\frac{x}{x_i}\right)^{D-1-\theta} \tag{2}$$

where $x_i$ is the reference location at the primary fracture face, ft; $x$ is the distance away from the primary fracture face, ft; $\phi_i$ is the initial porosity at the reference position, fraction; $k_i$ is the initial permeability at the reference position, mD; $D$ is the fractal dimension used to quantify the extent of reservoir heterogeneity; and $\theta$ is the fluid anomalous diffusion exponent caused by heterogeneity (Ozcan et al., 2014). The diffusion equations describing multiphase fluid flow through a reservoir with non-uniform distribution of permeability and porosity in space are as follows:

Gas:

$$\frac{\partial}{\partial x}\left[ak(x)\frac{\partial p}{\partial x}\right] = \phi(x)\frac{\partial b}{\partial t}. \tag{3}$$

Oil:

$$\frac{\partial}{\partial x}\left[\alpha k(x)\frac{\partial p}{\partial x}\right] = \phi(x)\frac{\partial \beta}{\partial t} \tag{4}$$

Water:

$$\frac{\partial}{\partial x}\left[\gamma k(x)\frac{\partial p}{\partial x}\right] = \phi(x)\frac{\partial \xi}{\partial t} \tag{5}$$

where $p$ is pressure; $t$ is time; $a$ and $b$ are the simplified notations for gas flow equation related to pressure and saturations, $a = \frac{k_{rg}}{\mu_g B_g} + \frac{R_s k_{ro}}{\mu_o B_o}$, $b = \frac{S_g}{B_g} + \frac{R_s S_o}{B_o}$; $\alpha$ and $\beta$ are the simplified notations for oil flow equation related to pressure and saturations, $\alpha = \frac{k_{ro}}{\mu_o B_o} + \frac{R_v k_{rg}}{\mu_g B_g}$, $\beta = \frac{S_o}{B_o} + \frac{R_v S_g}{B_g}$; $\gamma$ and $\xi$ are the simplified notations for water flow equation related to pressure and saturations, $\gamma = \frac{k_{rw}}{\mu_w B_w}$, $\xi = \frac{S_w}{B_w}$. The mathematical notations are consistent with those of Hamdi et al. (2018). $B_g$, $B_o$, $B_w$ are the formation volume factors for gas, oil and water; $\mu_g$, $\mu_o$, $\mu_w$ are the viscosities of gas, oil and water; $S_g$, $S_o$, $S_w$ are the gas, oil and water saturation, respectively; $k_{rg}$, $k_{ro}$, $k_{rw}$ are the gas, oil and water relative permeability, respectively; $R_s$ is the solution gas to oil ratio; $R_v$ is the vaporized oil to gas ratio.

In this work, rock compressibility and capillary pressure are neglected, which is the conventional assumption in analytical multiphase flow analysis methods (Hamdi et al., 2018). In addition, the rock and fluid parameters utilize the following assumptions:

1. $B_g(p)$, $B_o(p)$, $\mu_g(p)$, $\mu_o(p)$, $R_s(p)$, $R_v(p)$ are functions of pressure.
2. $k_{rw}(S_w)$, $k_{rg}(S_g)$ are functions of the corresponding phase saturations while $k_{ro}(S_w, S_g)$ is a function of two-phase saturations and calculated using Stone's first model (Stone, 1973).

The conventional Boltzmann variable can be used to reduce the number of variables for cases with uniform permeability and porosity distribution. However, for the diffusion equations corresponding to heterogeneous reservoirs (Eqs. (3)–(5)), the conventional Boltzmann variable cannot play the same role when permeability and porosity are varying in space. To address this issue, for the first time, a new Boltzmann-type variable (Eq. (6)) is proposed using the method of undetermined coefficients (Stelson, 1950). The details are provided in Appendix A.

$$\eta = \sqrt{\frac{\phi_i}{k_i}} x_i^{D-1-\theta} x^{2+\theta-D} t^{\frac{D-2-\theta}{2+\theta}}. \tag{6}$$

where $\eta$ is the modified Boltzmann variable.

The type of Boltzmann variable could be simplified to be the conventional Boltzmann variable that appears in Hamdi et al. (2018) when reservoir is homogenous ($D = 1$, $\theta = 0$; $\eta = x(\phi/kt)^{0.5}$). Through application of this new Boltzmann variable, the original three-phase fluid flow PDEs are transformed to ordinary differential equations (ODE's) as follows:

Gas:

$$\frac{d}{d\eta}\left(a\frac{dp}{d\eta}\right) = w\eta^c \frac{db}{d\eta}. \tag{7}$$

Oil:

$$\frac{d}{d\eta}\left(\alpha\frac{dp}{d\eta}\right) = w\eta^c \frac{d\beta}{d\eta}. \tag{8}$$

Water:

$$\frac{d}{d\eta}\left(\gamma\frac{dp}{d\eta}\right) = w\eta^c \frac{d\xi}{d\eta}. \tag{9}$$

where $w$ and $c$ are intermediate variables used to simplify the expression of the above equations:

$$w = -\frac{1}{(2+\theta-D)(2+\theta)}\left(\frac{\phi_i}{k_i}\right)^{\frac{1-c}{2}} x_i^{(c+1)(1-D)+c\theta}. \tag{10}$$

$$c = \frac{D}{2+\theta-D}. \tag{11}$$

Three-phase parameters in Eqs. (7)–(9) ($a$, $b$, $\alpha$, $\beta$, $\gamma$, $\xi$) are functions of pressure and the phase saturations, e.g., $\alpha = f(p, S_w, S_g)$. Hence, as an example, the total differential of $\alpha$ can be expressed as follows:

$$d\alpha = \left(\frac{\partial \alpha}{\partial p}\right)_{S_w,S_g} dp + \left(\frac{\partial \alpha}{\partial S_w}\right)_{p,S_g} dS_w + \left(\frac{\partial \alpha}{\partial S_g}\right)_{p,S_w} dS_g. \tag{12}$$

For ease of simple expression, Eq. (12) can be further simplified to be Eq. (13):

$$d\alpha = \alpha_1 dp + \alpha_2 dS_w + \alpha_3 dS_g. \tag{13}$$

The total differentials for other variables ($a$, $b$, $\beta$, $\gamma$, $\xi$) are derived in a similar fashion as Eq. (13), the details of which are provided in

Appendix B. After a series of mathematical derivations shown in Appendix B, the equations describing water saturation and gas saturation gradients with respect to the new Boltzmann variable can be obtained as follows, respectively.

$$\frac{dS_w}{d\eta} = -\frac{dS_g}{d\eta}\left[\frac{\frac{dp}{d\eta}(\alpha a_3 - a\alpha_3) - w\eta^c(\alpha b_3 - a\beta_3)}{\frac{dp}{d\eta}(\alpha a_2 - a\alpha_2) - w\eta^c(\alpha b_2 - a\beta_2)}\right] - \frac{dp}{d\eta}\left[\frac{\frac{dp}{d\eta}(\alpha a_1 - a\alpha_1) - w\eta^c(\alpha b_1 - a\beta_1)}{\frac{dp}{d\eta}(\alpha a_2 - a\alpha_2) - w\eta^c(\alpha b_2 - a\beta_2)}\right]. \quad (14)$$

$$\frac{dS_g}{d\eta} = \frac{dp}{d\eta}\frac{\frac{\frac{dp}{d\eta}(\alpha\gamma_1 - \gamma\alpha_1) - w\eta^c(\alpha\xi_1 - \gamma\beta_1)}{\frac{dp}{d\eta}(\alpha\gamma_2 - \gamma\alpha_2) - w\eta^c(\alpha\xi_2 - \gamma\beta_2)} - \frac{\frac{dp}{d\eta}(\alpha a_1 - a\alpha_1) - w\eta^c(\alpha b_1 - a\beta_1)}{\frac{dp}{d\eta}(\alpha a_2 - a\alpha_2) - w\eta^c(\alpha b_2 - a\beta_2)}}{-\frac{\frac{dp}{d\eta}(\alpha\gamma_3 - \gamma\alpha_3) - w\eta^c(\alpha\xi_3 - \gamma\beta_3)}{\frac{dp}{d\eta}(\alpha\gamma_2 - \gamma\alpha_2) - w\eta^c(\alpha\xi_2 - \gamma\beta_2)} + \frac{\frac{dp}{d\eta}(\alpha a_3 - a\alpha_3) - w\eta^c(\alpha b_3 - a\beta_3)}{\frac{dp}{d\eta}(\alpha a_2 - a\alpha_2) - w\eta^c(\alpha b_2 - a\beta_2)}}. \quad (15)$$

Eqs. (14) and (15) are non-linear ODEs including rock and fluid properties and pressure gradient. Following the work of Zhang et al. (2014) and Hamdi et al. (2018), the Rung-Kutta (RK) method is also employed to solve the transformed governing flow equations (Eqs. (7)–(9)) rigorously. For this purpose, Eqs. (14) and (15) can provide the solutions of water and gas saturation in differential form. In addition, the pressure gradient for the Boltzmann variable ($\eta$) is required for capturing spatial and temporal pressure changes in reservoir. However, because Eq. (8) is a second order ODE, an extra ordinary differential variable (pressure gradient: $p_d = \alpha dp/d\eta$) is needed for order reduction, which is necessary for the solution. As a consequence, four ordinary differential equations ($dp/d\eta$, $dS_w/d\eta$, $dS_g/d\eta$, $dp_d/d\eta$) are developed as follows with their boundary conditions:

$$\begin{cases} \frac{dp}{d\eta} = \frac{1}{\alpha}p_d \quad p|_{\eta=0} = p_{wf}\ ;\ \ p|_{\eta=\infty} = p_i \quad \text{(a)} \\ \frac{dS_w}{d\eta} = \text{Eq. 14} \quad S_w|_{\eta=\infty} = S_{wi} \quad \text{(b)} \\ \frac{dS_g}{d\eta} = \text{Eq.15} \quad S_g|_{\eta=\infty} = S_{gi} \quad \text{(c)} \\ \frac{dp_d}{d\eta} = w\eta^c\frac{d\beta(p, s_w, s_g)}{d\eta} \quad \text{(d)} \end{cases}. \quad (16)$$

where $p_{wf}$ is flowing bottom hole pressure; $w$ and $c$ are related with $D$ and $\theta$ that can be dealt with constant values. As evident from Eq. (16), the initial conditions of the reservoir are the same as the corresponding outer boundary of pressure and saturations. In Eq. (16a), introduction of $p_d$ helps overcome the issue of pressure solution to satisfy two boundary conditions. To find a consistent solution for Eq. (16), $p|_{\eta=\infty} = p_i$ is used as the primary boundary condition; as a result, an input value (usually a very small number) is then required for $p_d$ at $\eta = \infty$ in such a way that the pressure solution can satisfy another boundary condition, i.e., $p|_{\eta=0} = p_{wf}$. This is achieved by using a trial-and-error approach based on the Bisection method, which can find values of $p_d$ at the outer boundary quickly. Then, the analytical solution for Eq. (16) can be found to determine the distribution profile of pressure and phase saturations as functions of the new Boltzmann variable.

### 2.2. RTA application

As described above, both the transient saturation–pressure relationship and transient linear flow solution for the constant flowing bottom hole pressure case are obtained using the new Boltzmann-type transformation. For three-phase flow in heterogeneous reservoirs with AD effects, Eq. (17) is the transient rate equation for the oil phase obtained using Darcy's law:

$$q_o = k\alpha(p, S_w, S_g)A\left(\frac{dp}{dx}\right)_{x=0}. \quad (17)$$

where $q_o$ is the oil rate, $m^3$/day; $A$ is the cross sectional area, $m^2$. Using the new Boltzmann variable (Eq. (6)), Eq. (17) can be further transformed as follows:

$$q_o = A_1 2x_f h\sqrt{k_i\phi_i}(2 + \theta - D)p_d|_{\eta=0}(A_2 t)^{\frac{D-2-\theta}{2+\theta}}. \quad (18)$$

where $A_1$, $A_2$ are both the unit conversion factors for metric units ($A_1 = 27.32$; $A_2 = 86400$); $x_f$ is the effective fracture half-length, m; $h$ is the reservoir thickness, m; $t$ is the production time, day; $p_d|_{\eta=0}$ can be calculated from the set of ODE's where $\phi_i$, $h$, $D$ and $\theta$ must be known. Knowing the pressure, gas and water saturations, $\alpha$, $a$ and $\gamma$ can be calculated. The pressure gradient $(dp/d\eta)_{\eta=0}$ can be estimated further which means that Eq. (18) can rewrite for water and gas phase as follows:

$$q_g = A_1 2x_f h\sqrt{k_i\phi_i}(2 + \theta - D)a\left.\frac{dp}{d\eta}\right|_{\eta=0}(A_2 t)^{\frac{D-2-\theta}{2+\theta}}. \quad (19)$$

$$q_w = A_1 2x_f h\sqrt{k_i\phi_i}(2 + \theta - D)\gamma\left.\frac{dp}{d\eta}\right|_{\eta=0}(A_2 t)^{\frac{D-2-\theta}{2+\theta}}. \quad (20)$$

where $q_g$ is the gas rate, $m^3$/day; $q_w$ is the water rate, $m^3$/day.

In contrast to the classical square-root-of-time plot, which cannot be used for this case due to the impact of reservoir heterogeneity and anomalous diffusion, Eq. (18) can be used to develop a time-power-law-plot of $1/q_o$ versus $t^{(2+\theta-D)/(2+\theta)}$ whose slope can be expressed as $2x_f h(k_i\phi_i)^{0.5}(2 + \theta - D)p_d\big|_{\eta=0}$. As a result, the linear flow parameter $(x_f k_i^{0.5})$ can be estimated from the new time-power-law plot for the case of reservoir heterogeneity and anomalous diffusion. Fig. 1 provides the step-wise workflow to calculate $x_f k_i^{0.5}$ for TLF for wells flowing at constant flowing bottom hole pressure conditions.

The workflow is summarized as follows:

Step 1: Gather the basic data for analysis including production rates of different phases, bottom hole flowing pressure, relative permeability curves, fluid PVT, matrix permeability and porosity.

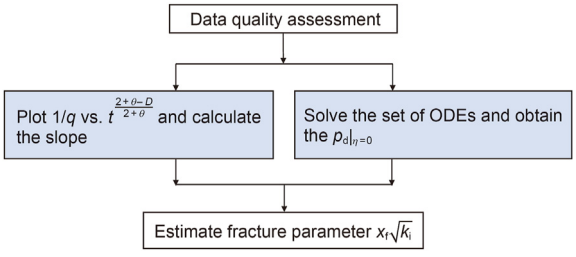


**Fig. 1.** A step-wise workflow to estimate the linear flow parameter for multiphase transient linear flow in heterogeneous reservoirs with anomalous diffusion effects.

Step 2: Solve the analytical model for multiphase transient linear flow in heterogeneous reservoirs by using the Runge-Kutta method to obtain $p_d|_{\eta=0}$.
Step 3: Plot $1/q_o$ versus $t^{(2+\theta-D)/(2+\theta)}$ and evaluate the slope of the observed straight-line.
Step 4: Estimate the linear flow parameter, $x_f k_i^{0.5}$, using the slope and $p_d|_{\eta=0}$.

## 3. Results

In this section, the new analytical model and RTA workflow are applied to a simulation case. Next, the model is applied to a field case to demonstrate practical application.

### 3.1. Model verification with numerical simulation

In this section, the new analytical model and RTA workflow are applied to a simulation case. The simulation model (Fig. 2) is designed to simulate the TLF regime, and all hydraulic fractures are assumed symmetrical with infinite conductivity. To reduce simulation runtimes, an element of symmetry (single fracture stage) model is applied, and then scaled up to a MFHW with the full number of stages. To obtain accurate pressure and phase saturation distributions, the grid blocks are refined in the near-fracture-face region, as shown in Fig. 3. The well is operated under a constant bottom hole pressure (10 MPa) condition.

To illustrate the impacts of reservoir heterogeneity and AD, fractal theory is applied, where the fractal dimension is 0.7 and AD exponent is 0.5. Fig. 4 presents the fractal-based non-uniform distribution of matrix reservoir permeability and porosity, where the reference permeability and porosity at the fracture face are 0.01 mD and 10%, respectively. Table 1 summarizes the other key input parameters used to construct the simulation model. The relative permeability is calculated in Brooks-Corey equation (Christiansen and Lake, 2007), the input parameters are listed in Table 2.

In this work, a black-oil model is applied. The simulated reservoir is at a depth of 1500 m with initial temperature of 50 °C and initial pressure of 28.6 MPa. The initial water saturation in the reservoir is 0.45, which is greater than the connate water saturation, $S_{wc} = 0.2$. The relative permeability curves are generated with Brooks–Corey equations (Christiansen and Lake, 2007). It should be noted that the oil-phase relative permeability is calculated using Stone's first model(Stone, 1973), $k_{ro} = f(S_w, S_g)$. The PVT properties used in the simulation model are illustrated in Fig. 5.

Fig. 6a–c compares the pressure, gas saturation and oil saturation paths versus Boltzmann variable for both the numerical simulation model and analytical model. The results demonstrate good agreement between both models for the case of multiphase transient linear flow in heterogeneous reservoirs with anomalous diffusion. Differences between pressure and saturation for the two methods are within 5%. In addition, by eliminating the Boltzmann variable, the saturation–pressure relationship can be obtained. The gas saturation–pressure and oil saturation–pressure relationships are illustrated in Fig. 7a and b, respectively. The S–P path is an essential input for RTA using the modified pseudo-variable

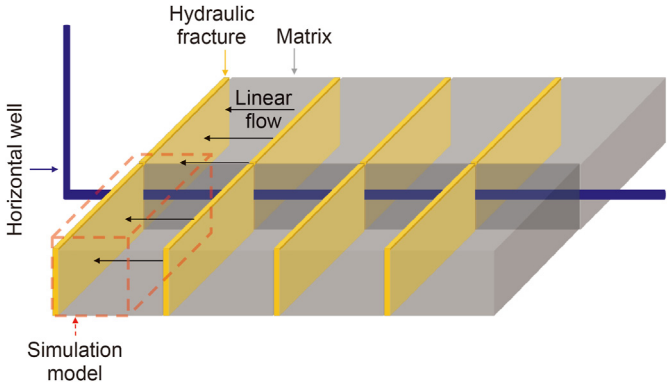


**Fig. 2.** Illustration of a MFHW and the element of symmetry used for simulation modelling.


**Fig. 3.** Gridblock pressures at early time generated using the reservoir simulation model.

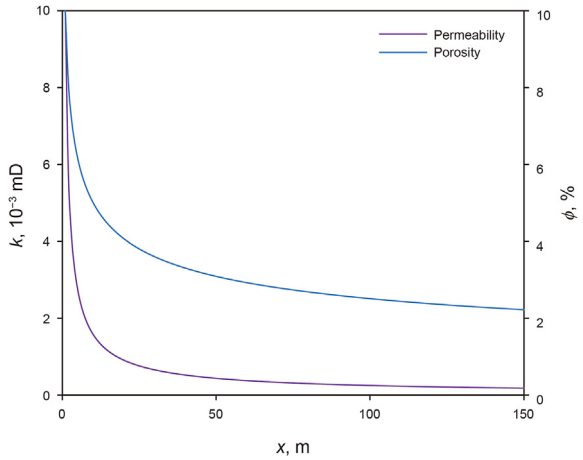


**Fig. 4.** Non-uniform distribution of permeability and porosity generated using fractal theory, where the fractal dimension is 0.7 and anomalous diffusion exponent is 0.5.

**Table 1**
Key input parameters of reservoir simulation model.

| Parameter | Value | Parameter | Value |
|---|---|---|---|
| Reference porosity | 10% | Thickness | 10 m |
| Reference permeability | 0.01 mD | Initial reservoir pressure | 28.6 MPa |
| Fracture half-length | 152 m | Bubble point pressure | 28.6 MPa |
| Fractal dimension | 0.7 | Anomalous diffusion exponent | 0.5 |

**Table 2**
Parameters for Brooks-Corey equations to calculate relative permeability.

| $n_{ow}$ | $n_w$ | $n_g$ | $n_{og}$ | $k_{rwmax}$ | $k_{rgmax}$ | $S_{gc}$ | $S_{wc}$ | $S_{org}$ | $S_{orw}$ |
|---|---|---|---|---|---|---|---|---|---|
| **3** | 3 | 3 | 3 | 0.2 | 0.2 | 0 | 0.2 | 0.1 | 0.1 |

*Note*: $n_{ow}$, $n_w$ are Brooks-Corey exponents for oil and water relative permeability in oil-water system, dimensionless; $n_{og}$, $n_g$ are Brooks-Corey exponents for oil and gas relative permeability in oil-gas system, dimensionless; $k_{rw\_max}$, $k_{rg\_max}$ are the maximum water and gas relative permeability respectively, dimensionless; $S_{wc}$ and $S_{gc}$ are the critical water and gas saturation, dimensionless; $S_{orw}$ and $S_{org}$ are residual oil saturation in oil-water system and oil-gas system, dimensionless.

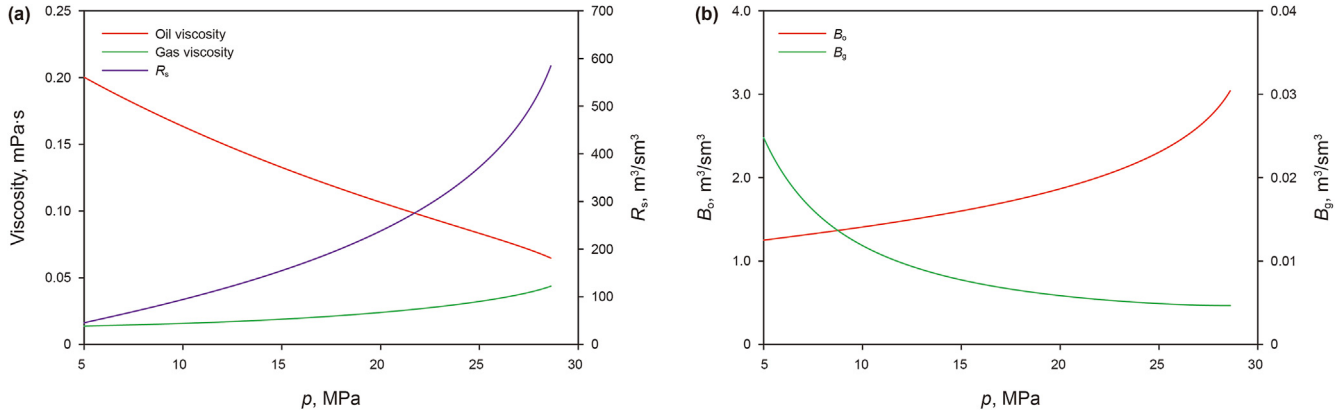


**Fig. 5.** PVT properties used in simulation model: (**a**) oil and gas viscosity, solution gas to oil ratio; (**b**) formation volume factors for oil and gas.

approach, as discussed by Hamdi et al. (2018).

As described in the previous section, the value of $p_d$ at $\eta = 0$, and the slope of straight-line analysis plot, can be employed to estimate the linear flow parameter $x_f k_i^{0.5}$. Fig. 8a provides the classical square-root-of-time plot analysis (with the assumption of a homogeneous reservoir) using the transient linear flow solution of Wattenbarger et al. (1998). From this plot, the linear flow parameter, $x_f k_i^{0.5}$, is estimated to be 5.77 m·mD$^{0.5}$, which is much smaller than the value input into the simulator (15.20 m·mD$^{0.5}$). In contrast, the new time-power-law-plot (that is, $1/q_o$ vs. $t^{0.72}$ in this case), which incorporates the impacts of reservoir heterogeneity and multiphase flow, is shown in Fig. 8b. Using the slope of the straight line of the time-power-law plot, the linear-flow-parameter $x_f k_i^{0.5}$ is estimated to be 15.51 m·mD$^{0.5}$, which is within 2% of the simulation input. As a result, it is necessary to consider the impacts of multiphase flow and reservoir heterogeneity when it occurs.

### 3.2. Model application to field data

In this section, practical application of the new model is demonstrated using a hydraulically-fractured horizontal well located in the Junggar Basin. The target reservoir has an initial reservoir pressure of 71.3 MPa, reservoir temperature of 105 °C, and a net play of 7 m. The relative densities of crude oil and gas measured in the laboratory are 0.83 and 0.78, respectively. Fig. 9 provides some of the additional well data and PVT properties calculated using the empirical formulas constrained by experimental data. In this work, the relative permeability curves are fitted to laboratory data using Brooks-Corey equations (Christiansen and Lake, 2007) with the resulting parameters reported in Table 3. From Fig. 10, it is observed that BHP declined substantially at early time, after which (approximately 20 days) BHP stayed constant about 46 MPa. In this work, the degree of reservoir heterogeneity is estimated through slope of oil production versus time on a log-log plot, resulting in $D = 0.85$ and $\theta = 0$. Fig. 11 provides the comparison of rate-transient analysis using the classical square-root-of-time plot (with the assumption of a homogeneous reservoir) and the new time-power-law-plot (that is, $1/q_o$ vs. $t^{0.575}$ in this case, of which the power-law exponent is calculated using Eq. (18) with the original simulation inputs). The fracture half-length, $x_f$, is estimated to be 43.76 m (within 47.3% in error with the original input) using the classical transient linear flow analysis. In comparison, the novel time-power-law-plot incorporates the impacts of reservoir heterogeneity and multiphase flow. Using the slope of the straight line of the time-power-law plot, the fracture half-length $x_f$ is estimated

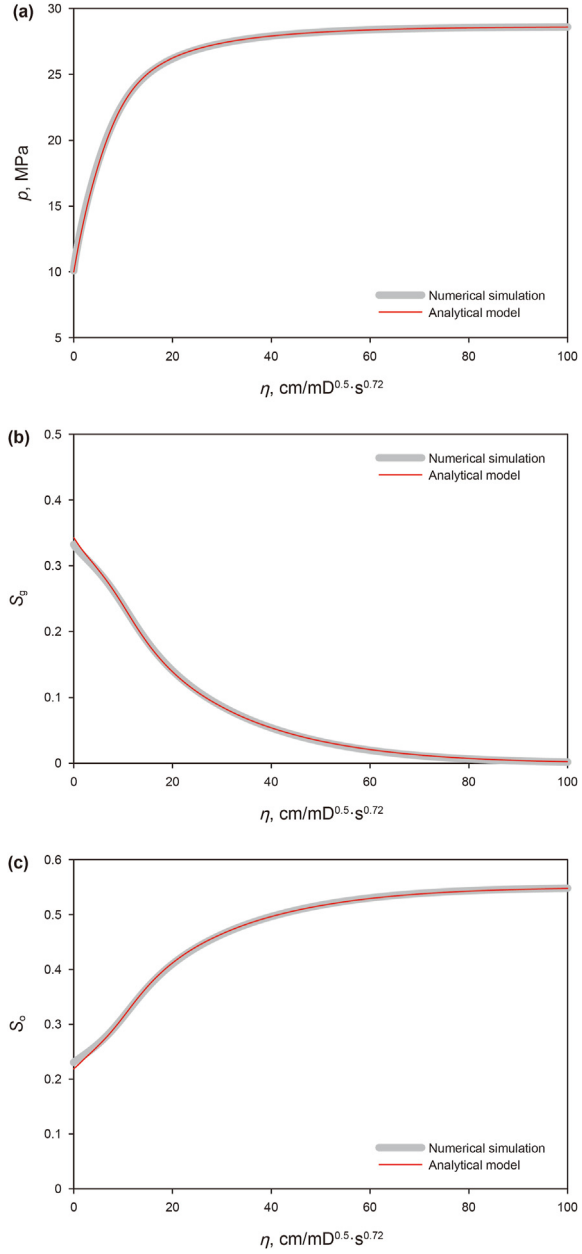


**Fig. 6.** Comparisons of pressure, water saturation and oil saturation paths obtained from the fine-grid numerical simulation and the analytical solution: (**a**) pressure versus Boltzmann variable; (**b**) gas saturation versus Boltzmann variable; (**c**) oil saturation versus Boltzmann variable.

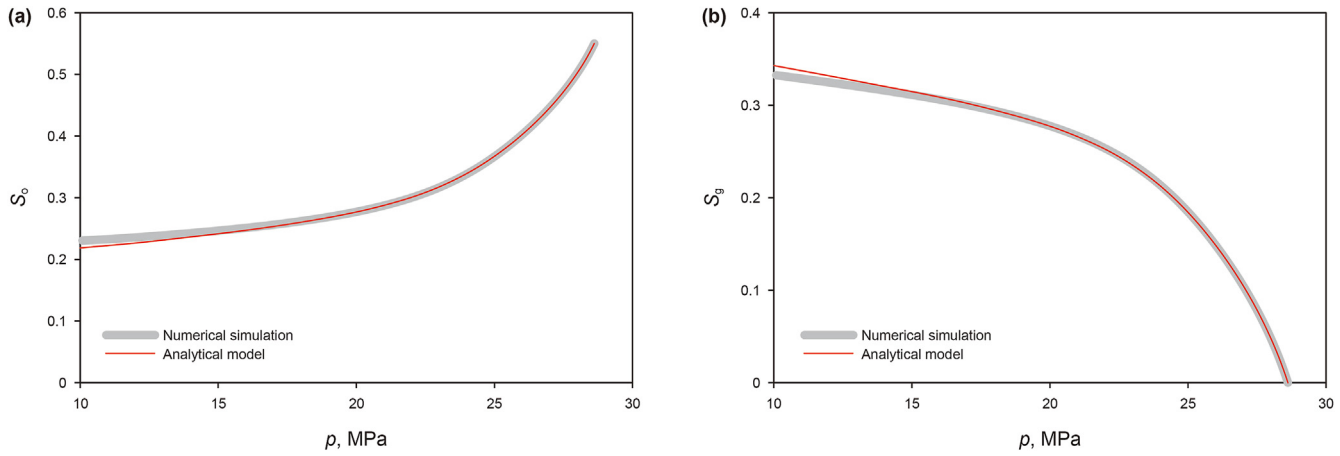


**Fig. 7.** Oil (**a**) and gas (**b**) saturation–pressure relationships obtained from numerical simulation and analytical model.

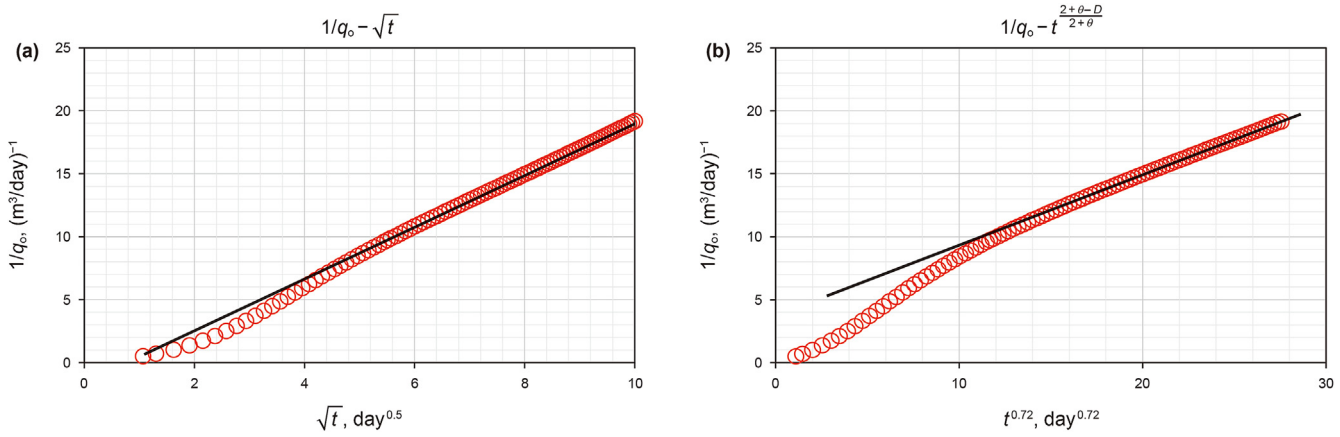


**Fig. 8.** Conventional square-root-of-time plot (**a**) and improved time-power-law plot (**b**). The latter can be used to evaluate the linear flow parameter for a heterogeneous reservoir with multiphase flow.

to be 85.3 m, which is within 2.8% of the value of history-matched simulation case. Fig. 12 shows results of history matching oil/gas rates and cumulative production using the analytical model. The history-matching error of the cumulative production is within 3%.

## 4. Discussion

After successful validation of the new semi-analytical model using numerical simulation, and practical application of the model

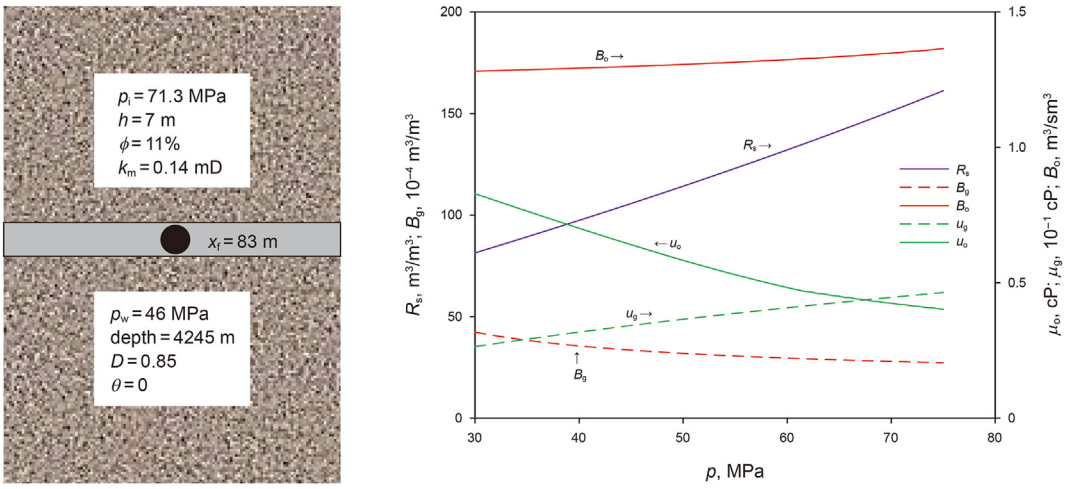


**Fig. 9.** Data used for field case analysis: (**a**) schematic of studied well with additional input data, (**b**) multiphase fluid PVT properties.

**Table 3**
Brooks-Corey parameters used to calculate relative permeability.

| $n_{ow}$ | $n_w$ | $n_g$ | $n_{og}$ | $k_{rwmax}$ | $k_{rgmax}$ | $S_{gc}$ | $S_{wc}$ | $S_{org}$ | $S_{orw}$ |
|---|---|---|---|---|---|---|---|---|---|
| **2.5** | 1 | 1.5 | 3 | 0.1 | 0.7 | 0 | 0.2 | 0.15 | 0.15 |

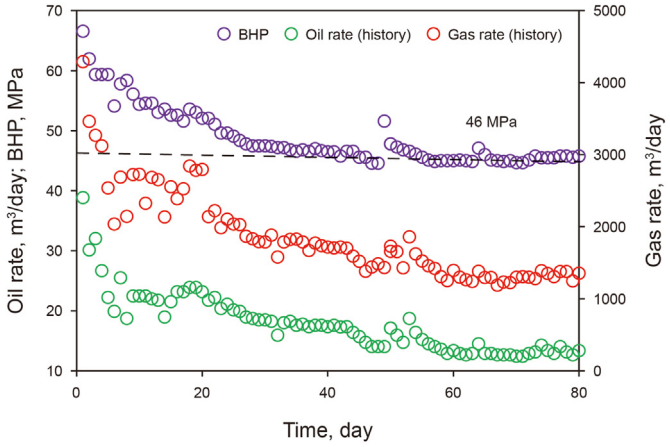


**Fig. 10.** Production rates (oil & gas) and flowing bottom hole pressures (BHPs) for target well in the Junggar Basin.

to field data, a sensitivity study was performed to evaluate the impacts of multiphase flow, reservoir geometric heterogeneity and anomalous diffusion on the rate-decline behavior respectively.

It is quite common for MFHWs completed in tight oil reservoirs to exhibit power-law behavior on log-log diagnostic plots (Chu et al., 2019), as described with the equation $q_o = q_{ini}t^{-n}$ where $q_{ini}$ is the initial oil production rate, $m^3$/day, and $n$ is the power-law exponent, dimensionless. The new analytical model (Eq. (18)) also predicts power-law behavior. Hence, the initial oil production rate and production rate-decline exponent constant can be expressed as shown in Eq. (21a, b). The detailed derivation can be found in Appendix C.

Initial oil production rate:

$$q_{ini} = A_1 2x_f h\sqrt{k_i\phi_i}(2+\theta-D)p_d|_{\eta=0}A_2^{\frac{D-2-\theta}{2+\theta}} \tag{21a}$$

Production decline exponent constant:

$$b = \frac{1}{n} = \frac{2+\theta}{2+\theta-D} \tag{21b}$$

Using these relationships, the impact of multiphase flow on initial oil rate, and the impacts of reservoir heterogeneity/rate-decline behavior, can now be explored using the new model.

### 4.1. Impact of multiphase flow on initial oil production rate

As shown in Eq. (21a, b), multiphase flow only affects the initial oil production rate and does not affect the production decline exponent constant. In this work, the impact of multiphase flow is

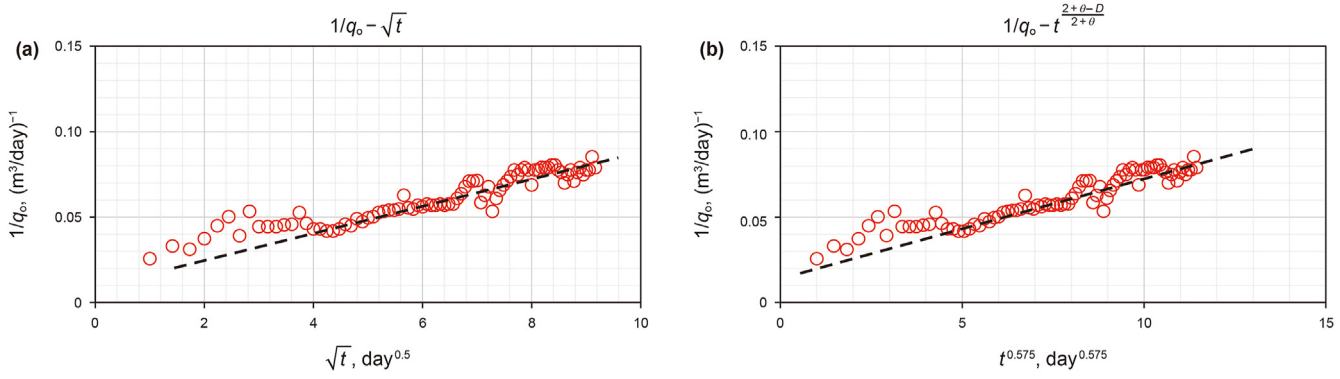


**Fig. 11.** Conventional square-root-of-time plot (**a**) and improved time-power-law plot (**b**). The latter can be used to evaluate the linear flow parameter for a heterogeneous reservoir with multiphase flow.

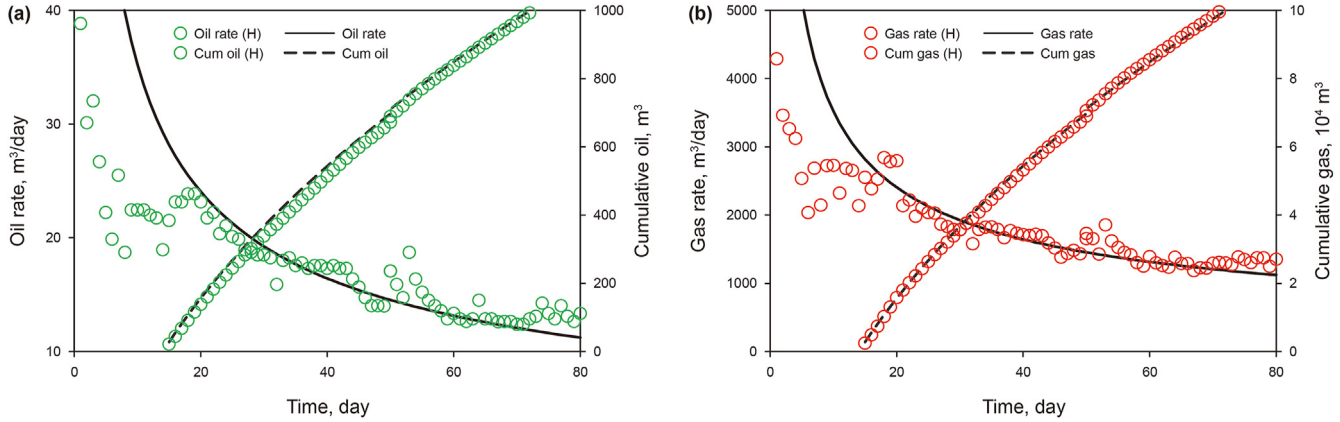


**Fig. 12.** History matching results for oil production rate and cumulative oil production (**a**) and gas production rate and cumulative gas production (**b**). In this plot "H" denotes the history or measured datapoints and "Cum" is abbreviation for cumulative production.

investigated using different oil/water relative permeability curves. The BrooksCorey equation parameters are varied (see Table 4 for model inputs) while all other input parameters are same as those applied to the simulation model used for verification. As shown in Fig. 13a and b, the values of initial oil rate in the rate–decline model increase with the ehancement of oil mobility (i.e. as $n_{ow}$ and $n_{og}$ decrease). In contrast, the initial oil production rate drops with an increase of gas/water mobility (i.e., as $n_g$ decreases, in Fig. 13c; as $k_{rgmax}$, $k_{rwmax}$ increase, in Fig. 13d and e), and it is noted that the impact of water mobility has a minor impact on the initial oil production rates (Fig. 13d). Compared to water production, the enhancement of gas production has more significant impact on the initial oil production rate (i.e., the impacts of $n_{og}$ vs. $n_{ow}$, Fig. 13a vs. Fig. 13b; the impact of $k_{rgmax}$ vs. $k_{rwmax}$, Fig. 13d vs. Fig. 13e).

**Table 4**
Summary of the input values for different Brooks-Corey equation parameters used for sensitivity study.

| Input parameters | Value range |
|---|---|
| Case a: $n_{ow}$ | 1–4 |
| Case b: $n_{og}$ | 1–4 |
| Case c: $n_g$ | 1–4 |
| Case d: $k_{rwmax}$ | 0.2–0.8 |
| Case e: $k_{rgmax}$ | 0.2–0.8 |

### 4.2. Impact of reservoir heterogeneity/anomalous diffusion on rate decline behavior

To study these effects, different fractal dimension and anomalous diffusion exponents are used (see Table 5) in the simulation model while fluid properties are consistent with values used in verification section. As suggested from Eq. (19), reservoir

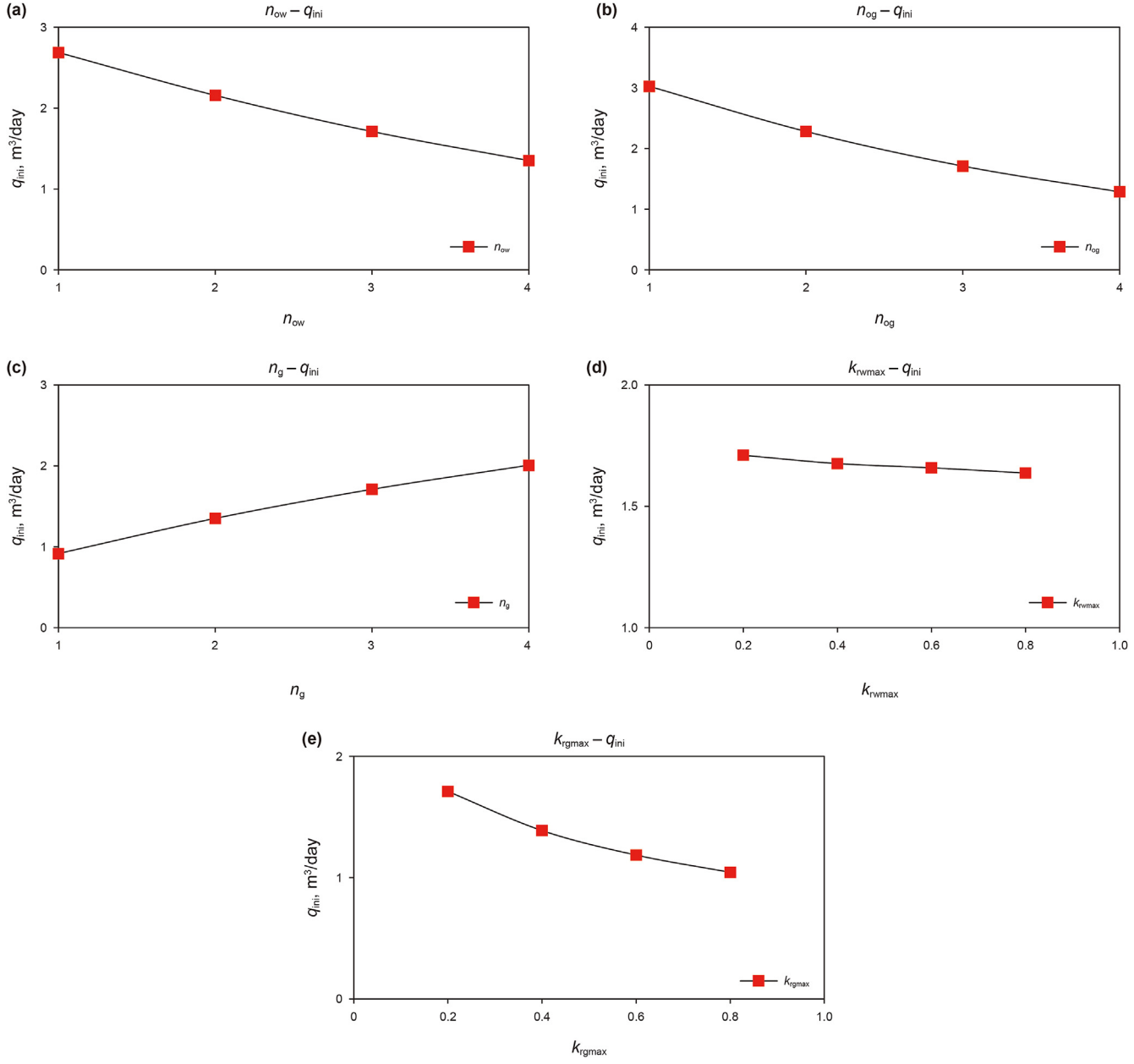


**Fig. 13.** Impact of multiphase flow (using BrooksCorey equations) on the initial oil production rate ($q_{ini}$): (**a**) $n_{ow}$, (**b**) $n_{og}$, (**c**) $n_g$, (**d**) $k_{rwmax}$, (**e**) $k_{rgmax}$.

**Table 5**
Summary of the input values for fractal dimension and anomalous diffusion exponents used in sensitivity study.

| Case | Fracture dimension $D$ | Anomalous diffusion exponent $\theta$ |
|---|---|---|
| Case a | 0.2–0.8 | 0 |
| Case b | 0.2–0.8 | 0.2 |
| Case c | 0.2–0.8 | 0.5 |

heterogeneity/anomalous diffusion affect both the initial oil production rate and production decline exponent. Fig. 14 demonstrates that reservoir heterogeneity and anomalous diffusion have an obvious impact on $q_{ini}$. With a decrease of fractal dimension ($D$), the extent of reservoir heterogeneity is exaggerated; as a result, the initial oil production rate decreases. With an increase in the anomalous diffusion exponent ($\theta$), the resistance to fluid flow (caused by reservoir heterogeneity) increases, also leading to a drop of initial oil production. Fig. 15 suggests that, with an increase in reservoir heterogeneity and anomalous diffusion, the rate-decline exponent constant ($b$) follows a decreasing trend; that is, the decline of oil production is exaggerated. Furthermore, the impacts of reservoir heterogeneity on the production decline exponent are more evident than that of anomalous diffusion.

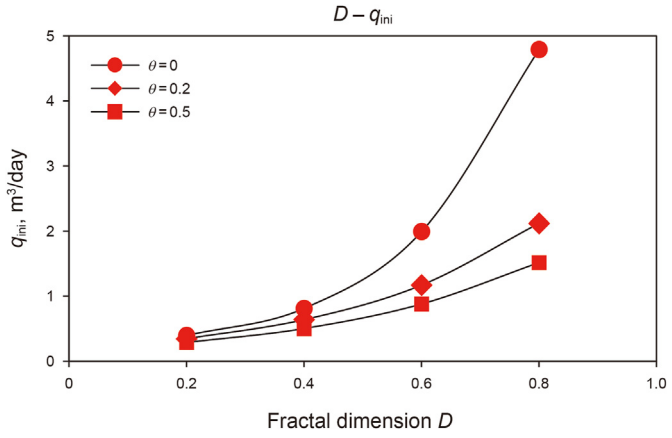


**Fig. 14.** Impact of reservoir heterogeneity and anomalous diffusion on the initial oil production rate $q_{ini}$.

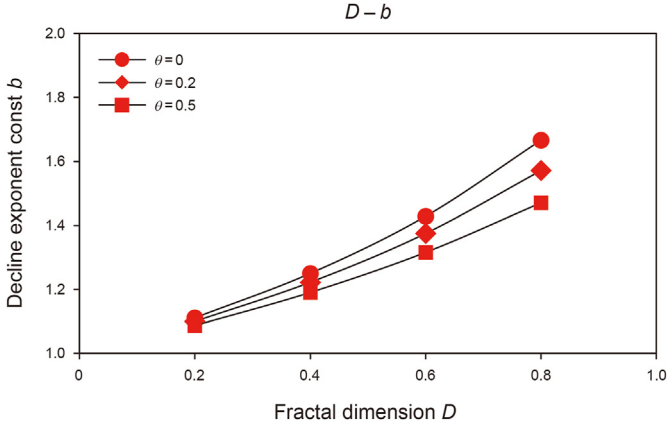


**Fig. 15.** Impact of reservoir heterogeneity and anomalous diffusion on the production decline exponent constant $b$.

## 5. Conclusions

In this work, a new semi-analytical model is developed that explicitly accounts for multiphase transient flow, fractal-based reservoir heterogeneity, anomalous diffusion (AD), and pressure-dependent fluid properties simultaneously. To derive the semi-analytical solution, a new Boltzmann-type variable is proposed, the exponent of which incorporate reservoir geometric heterogeneity and AD parameters. The new model is verified using fine-grid numerical reservoir simulation populated with light oil fluid properties. A new time-power-law plot is also proposed to estimate the reservoir and fracture properties, in recognition of the fact that the classical square-root-of-time-plot can result in misestimates when reservoir complexities are exhibited.

For the case of an approximately constant flowing pressure, multiphase flow has a significant effect on initial oil production rate, but has only a minor effect on the oil production decline exponent. Reservoir heterogeneity/anomalous diffusion affect both the initial oil production rate and production decline exponent. Moreover, the production decline exponent is a function of reservoir heterogeneity/anomalous diffusion alone.

The practical importance of this work is the advancement of analytical RTA models to allow for more complex reservoir scenarios, leading to more accurate production forecasting and better-informed capital planning. Future work will endeavor to improve the method for application to variable production conditions. This step will improve the practicality and rigorousness of the method of modified pseudo-variables for RTA applications.

## Acknowledgements

The authors would like to acknowledge financial support provided by National Natural Science Foundation of China (No. 52074338). We are also grateful to the support of the National Key R&D Program of China (No. 2019YFA0708700), and National Key Basic Research Program of China (20CX06071A). Bin Yuan would like to thank for the support of Shandong Mountain Tai Scholar Program. Chris Clarkson would like to acknowledge funding support from an NSERC Alliance grant (ALLRP 548652-19) for research related to the topic of this paper.

## Appendix A. Derivation of the new Boltzmann variable

Using the method of undetermined coefficients (Stelson, 1950), the new Boltzmann variable is determined as:

$$\eta = x^m k(x)^e \phi(x)^f t^n \tag{A-1}$$

where $m$, $e$, $f$, $n$ are undetermined exponents, fraction. Eq. A-1 can be written as Eq. A-2 through the fractal permeability and porosity equations:

$$\eta = k_i^e \phi_i^f x_i^{-(e+f)(D-1)+e\theta} x^{m+(e+f)(D-1)-e\theta} t^n \tag{A-2}$$

The left side of oil diffusion equation is $\frac{\partial}{\partial x}\left(k(x)\alpha\frac{\partial p}{\partial x}\right)$, which can be transformed as follows by using the new Boltzmann variable.

$$\frac{\partial}{\partial x}\left(k(x)\alpha\frac{\partial p}{\partial x}\right) = \frac{\partial}{\partial x}\left(Bx^{m+(e+f+1)(D-1)-(e+1)\theta-1} t^n \frac{dp}{d\eta}\right) \tag{A-3}$$

$$B = \alpha[m+(e+f)(D-1)-e\theta]k_i^{e+1}\phi_i^f x_i^{-(e+f+1)(D-1)+(e+1)\theta} \tag{A-4}$$

In Eq. A-4, $m+(e+f+1)(D-1)-(e+1)\theta-1$ should be zero to realize the reduction of equation order. To solve this equation, it is difficult and even not very necessary to find a general solution for the purpose of this work. Through using any unique solutions with different values of $m$, $e$, and $f$, different formulates of Boltzmann variables can be built, however, any types of unique solutions will lead to the same results of analytical solution of the original PDEs even with different formulates of Boltzmann variables. As a result, for the same of computational efficiency but without paying the prices of precision, a special unique solution is suggested with $m=1$, $e=-1$, $f=0$. The right side of oil diffusion equation is similarly converted using the new Boltzmann variable. The oil diffusion equation is transformed to be Eq. A-6 after some mathematical manipulations.

$$\eta = k_{\mathrm{i}}^{-1} x_i^{(D-1-\theta)} x^{2+\theta-D} t^n \tag{A-5}$$

$$\frac{\mathrm{d}}{\mathrm{d}\eta}\left(\alpha\frac{\mathrm{d}p}{\mathrm{d}\eta}\right) = \frac{n}{(2+\theta-D)^2} x_{\mathrm{i}}^{1-D} x^D t^{-n-1}\frac{\mathrm{d}\beta}{\mathrm{d}\eta} \tag{A-6}$$

In Eq. (A-6), $x^D t^{-n-1}$ is a power-law function of $\eta$ which follows $x^D t^{-n-1} = h\eta^c$; $k_{\mathrm{i}}$, $x_{\mathrm{i}}$ are constant. Therefore, $\left(\frac{\eta}{k_{\mathrm{i}}^{-1} x_{\mathrm{i}}^{D-1-\theta}}\right)^c = x^D t^{-n-1}$ is presented to calculate the unknown parameters.

$$x^{c(2+\theta-D)} t^{cn} = x^D t^{-n-1} \tag{A-7}$$

To make the space and time exponents consistent at both sides of equation, $c$ and $n$ become:

$$c = \frac{D}{2+\theta-D} \tag{A-8}$$

$$n = \frac{D-2-\theta}{2+\theta} \tag{A-9}$$

To be of similar form to the conventional Boltzmann variable at $D=1$, $\theta=0$, the new Boltzmann variable can be expressed as:

$$\eta = \sqrt{\frac{\phi_{\mathrm{i}}}{k_{\mathrm{i}}}} x_{\mathrm{i}}^{D-1-\theta} x^{2+\theta-D} t^{\frac{D-2-\theta}{2+\theta}} \tag{A-10}$$

## Appendix B. Derivation of water saturation and gas saturation gradients with respect to the new Boltzmann variable

The auxiliary variables used to simplify the ODE's are as follows:

$$N = \frac{\mathrm{d}p}{\mathrm{d}\eta},\ K = \frac{\mathrm{d}S_{\mathrm{w}}}{\mathrm{d}\eta},\ L = \frac{\mathrm{d}S_g}{\mathrm{d}\eta},\ \frac{K}{N} = \frac{\mathrm{d}S_w}{\mathrm{d}p},\ \frac{L}{N} = \frac{\mathrm{d}S_g}{\mathrm{d}p} \tag{B-1}$$

Using Eq. B-1, Eq. (8) can be written as:

$$N\left(\frac{\alpha_1\mathrm{d}p}{\mathrm{d}\eta}+\frac{\alpha_2\mathrm{d}S_{\mathrm{w}}}{\mathrm{d}\eta}+\frac{\alpha_3\mathrm{d}S_{\mathrm{g}}}{\mathrm{d}\eta}\right)+\alpha\frac{\mathrm{d}N}{\mathrm{d}\eta} = w\eta^c\left(\frac{\beta_1\mathrm{d}p}{\mathrm{d}\eta}+\frac{\beta_2\mathrm{d}S_{\mathrm{w}}}{\mathrm{d}\eta}+\frac{\beta_3\mathrm{d}S_{\mathrm{g}}}{\mathrm{d}\eta}\right) \tag{B-2}$$

$$N(\alpha_1 N+\alpha_2 K+\alpha_3 L)+\alpha\frac{\mathrm{d}N}{\mathrm{d}\eta} = w\eta^c(\beta_1 N+\beta_2 K+\beta_3 L) \tag{B-3}$$

Then the oil diffusion equation Eq. B-3 can be transformed as:

$$\alpha\frac{\mathrm{d}N}{\mathrm{d}\eta}+N(\alpha_1 N-w\eta^c\beta_1)+K(\alpha_2 N-w\eta^c\beta_2)+L(\alpha_3 N-w\eta^c\beta_3) = 0 \tag{B-4}$$

Gas and water diffusion equations can also transform to the following form:

$$a\frac{\mathrm{d}N}{\mathrm{d}\eta}+N(a_1 N-w\eta^c b_1)+K(a_2 N-w\eta^c b_2)+L(a_3 N-w\eta^c b_3) = 0 \tag{B-5}$$

$$\gamma\frac{\mathrm{d}N}{\mathrm{d}\eta}+N(\gamma_1 N-w\eta^c\xi_1)+K(\gamma_2 N-w\eta^c\xi_2)+L(\gamma_3 N-w\eta^c\xi_3) = 0 \tag{B-6}$$

$\mathrm{d}N/\mathrm{d}\eta$ is involved in three-phase flow equations. It can be eliminated by employing the oil equation Eq. B-4. As a result, the equation for $\mathrm{d}N/\mathrm{d}\eta$ is obtained as follows:

$$\frac{\mathrm{d}N}{\mathrm{d}\eta} = -\frac{1}{\alpha}[N(\alpha_1 N-w\eta^c\beta_1)+K(\alpha_2 N-w\eta^c\beta_2)+L(\alpha_3 N - w\eta^c\beta_3)] \tag{B-7}$$

Therefore, $\mathrm{d}N/\mathrm{d}\eta$ in gas flow equations can be written as:

$$a\left[-\frac{N}{\alpha}(\alpha_1 N-w\eta^c\beta_1)-\frac{K}{\alpha}(\alpha_2 N-w\eta^c\beta_2)-\frac{L}{\alpha}(\alpha_3 N-w\eta^c\beta_3)\right]+N(a_1 N-w\eta^c b_1)+K(a_2 N-w\eta^c b_2)+L(a_3 N-w\eta^c b_3) = 0 \tag{B-8}$$

Eq. B-8 can be multiplied by $\alpha/N$ as follows:

$$\left[-a(\alpha_1 N-w\eta^c\beta_1)-a\frac{K}{N}(\alpha_2 N-w\eta^c\beta_2)-a\frac{L}{N}(\alpha_3 N-w\eta^c\beta_3)\right]+\alpha(a_1 N-w\eta^c b_1)+\alpha\frac{K}{N}(a_2 N-w\eta^c b_2)+\alpha\frac{L}{N}(a_3 N-w\eta^c b_3) = 0 \tag{B-9}$$

After some mathematical manipulation, Eq. B-9 can be simplified as:

$$K = -\frac{L[N(\alpha a_3-a\alpha_3)-w\eta^c(\alpha b_3-a\beta_3)]+N[N(\alpha a_1-a\alpha_1)-w\eta^c(\alpha b_1-a\beta_1)]}{N(\alpha a_2-a\alpha_2)-w\eta^c(\alpha b_2-a\beta_2)} \tag{B-10}$$

Using Eq. B-1, Eq. B-10 can be written as follows:

$$\frac{dS_w}{d\eta} = -\frac{dS_g}{d\eta}\left[\frac{\frac{dp}{d\eta}(\alpha a_3 - a\alpha_3) - w\eta^c(\alpha b_3 - a\beta_3)}{\frac{dp}{d\eta}(\alpha a_2 - a\alpha_2) - w\eta^c(\alpha b_2 - a\beta_2)}\right] - \frac{dp}{d\eta}\left[\frac{\frac{dp}{d\eta}(\alpha a_1 - a\alpha_1) - w\eta^c(\alpha b_1 - a\beta_1)}{\frac{dp}{d\eta}(\alpha a_2 - a\alpha_2) - w\eta^c(\alpha b_2 - a\beta_2)}\right] \tag{B-11}$$

Similarly, the water phase flow equation can be transformed as follows:

$$\gamma\left[-\frac{N}{\alpha}(\alpha_1 N - w\eta^c\beta_1) - \frac{K}{\alpha}(\alpha_2 N - w\eta^c\beta_2) - \frac{L}{\alpha}(\alpha_3 N - w\eta^c\beta_3)\right] + N(\gamma_1 N - w\eta^c\xi_1) + K(\gamma_2 N - w\eta^c\xi_2) + L(\gamma_3 N - w\eta^c\xi_3) = 0 \tag{B-12}$$

Eq. B-12 can be multiplied by $\alpha/N$ as follows:

$$-\gamma(\alpha_1 N - w\eta^c\beta_1) - \gamma\frac{K}{N}(\alpha_2 N - w\eta^c\beta_2) - \gamma\frac{L}{N}(\alpha_3 N - w\eta^c\beta_3) + \alpha(\gamma_1 N - w\eta^c\xi_1) + \alpha\frac{K}{N}(\gamma_2 N - w\eta^c\xi_2) + \alpha\frac{L}{N}(\gamma_3 N - w\eta^c\xi_3) = 0 \tag{B-13}$$

After mathematic rearrangement, Eq. B-13 can be simplified as follows

$$K = -\frac{L[N(\alpha\gamma_3 - \gamma\alpha_3) - w\eta^c(\alpha\xi_3 - \gamma\beta_3)] + N[N(\alpha\gamma_1 - \gamma\alpha_1) - w\eta^c(\alpha\xi_1 - \gamma\beta_1)]}{N(\alpha\gamma_2 - \gamma\alpha_2) - w\eta^c(\alpha\xi_2 - \gamma\beta_2)} \tag{B-14}$$

Eq. B-10 and Eq. B-14 can be combined to obtain an ODE equation for gas saturation as follows:

$$\frac{dS_g}{d\eta} = \frac{dp}{d\eta}\frac{\frac{\frac{dp}{d\eta}(\alpha\gamma_1 - \gamma\alpha_1) - w\eta^c(\alpha\xi_1 - \gamma\beta_1)}{\frac{dp}{d\eta}(\alpha\gamma_2 - \gamma\alpha_2) - w\eta^c(\alpha\xi_2 - \gamma\beta_2)} - \frac{\frac{dp}{d\eta}(\alpha a_1 - a\alpha_1) - w\eta^c(\alpha b_1 - a\beta_1)}{\frac{dp}{d\eta}(\alpha a_2 - a\alpha_2) - w\eta^c(\alpha b_2 - a\beta_2)}}{-\frac{\frac{dp}{d\eta}(\alpha\gamma_3 - \gamma\alpha_3) - w\eta^c(\alpha\xi_3 - \gamma\beta_3)}{\frac{dp}{d\eta}(\alpha\gamma_2 - \gamma\alpha_2) - w\eta^c(\alpha\xi_2 - \gamma\beta_2)} + \frac{\frac{dp}{d\eta}(\alpha a_3 - a\alpha_3) - w\eta^c(\alpha b_3 - a\beta_3)}{\frac{dp}{d\eta}(\alpha a_2 - a\alpha_2) - w\eta^c(\alpha b_2 - a\beta_2)}} \tag{B-15}$$

For the case of oil and gas flow, the gas saturation gradient can be obtained by using Eq. B-11. It is noted that the differential variables for water are eliminated. Therefore, the gas saturation gradient is simplified as follows:

$$\frac{dS_g}{d\eta} = -\frac{dp}{d\eta}\frac{\frac{dp}{d\eta}(\alpha a_1 - a\alpha_1) - w\eta^c(\alpha b_1 - a\beta_1)}{\frac{dp}{d\eta}(\alpha a_3 - a\alpha_3) - w\eta^c(\alpha b_3 - a\beta_3)} \tag{B-16}$$

Similar mathematical manipulations can be performed for oil/water flow equations. The water saturation gradient is obtained as follows:

$$\frac{dS_w}{d\eta} = -\frac{dp}{d\eta}\frac{\frac{dp}{d\eta}(\alpha\gamma_1 - \gamma\alpha_1) - w\eta^c(\alpha\xi_1 - \gamma\beta_1)}{\frac{dp}{d\eta}(\alpha\gamma_2 - \gamma\alpha_2) - w\eta^c(\alpha\xi_2 - \gamma\beta_2)} \tag{B-17}$$

## Appendix-C. Derivation of rate-decline model to couple the impacts of multiphase flow, reservoir geometric heterogeneity and anomalous diffusion

The theory of all decline curve analysis begins with the concept of the nominal (instantaneous) decline rate $a_r$, which is defined as the fractional change in rate per unit time:

$$a_r = -\frac{\left(\frac{\Delta q}{q}\right)}{\Delta t} = -\frac{1}{q}\frac{\Delta q}{\Delta t} \tag{C-1}$$

Substituting the power-law production rate formula $q = q_{ini}t^{-n}$ into Eq. C-1 results in:

$$a_r = \frac{n}{t} \tag{C-2}$$

Another approach to representing the decline rate can be obtained by using the production rate $q$ and the decline exponent constant $b$:

$$a_r = Kq^b \tag{C-3}$$

As a result, the decline rate $a$ and production rate $q$ at any time satisfy the following relationship with initial decline rate $a_0$ and initial production rate $q_{ini}$:

$$\frac{a_r}{a_0} = \left(\frac{q}{q_{ini}}\right)^b \tag{C-4}$$

where $b$ is decline exponent constant. Eq. C-4 can be transformed as follows:

$$\frac{a_r}{a_0} = \frac{1}{t} = \left(\frac{q_{ini}t^{-n}}{q_{ini}}\right)^b = t^{-nb} \tag{C-5}$$

The production decline exponent constant $b$ is determined as follows:

$$b = \frac{1}{n} \tag{C-6}$$

## References


Acuña, J.A., 2016. Analytical pressure and rate transient models for analysis of complex fracture networks in tight reservoirs. SPE/AAPG/SEG Unconventional Resources Technology Conference. https://doi.org/10.15530/URTEC-2016-2429710.

Albinali, A., Ozkan, E., 2016. Anomalous diffusion approach and field application for fractured nano-porous reservoirs. In: SPE Annual Technical Conference and Exhibition. https://doi.org/10.2118/181255-MS.

Al-Rebeawi, S., 2019. Temporal and spatial anomalous diffusion flow mechanisms in structurally complex porous media: the impact on pressure behavior, flow regimes, and productivity index. In: Abu Dhabi International Petroleum Exhibition & Conference. https://doi.org/10.2118/197553-MS.

Artus, V., Houze, O., Chen, C.C., 2019. Flow regime-based decline curve for unconventional reservoirs: generalization to anomalous diffusion and power law behavior. SPE/AAPG/SEG Unconventional Resources Technology Conference. https://doi.org/10.15530/urtec-2019-293.

Behmanesh, H., Hamdi, H., Clarkson, C.R., 2015. Analysis of transient linear flow associated with hydraulically-fractured tight oil wells exhibiting multi-phase flow. In: SPE Middle East Unconventional Resources Conference and

Exhibition. https://doi.org/10.2118/SPE-172928-MS.
Behmanesh, H., 2016. Rate-transient Analysis of Tight Gas Condensate and Black Oil Wells Exhibiting Two-phase Flow. Ph.D. Dissertation. University of Calgary. https://doi.org/10.11575/PRISM/27534.
Boe, A., Skjaeveland, S.M., Whitson, C.H., 1989. Two-phase pressure test analysis. SPE Form. Eval. 4 (4), 604–610. https://doi.org/10.2118/10224-PA.
Christiansen, R.L., Lake, L.W., 2007. Relative Permeability and capillary Pressure. Petroleum engineering handbook: vol 1. In: Fanchi, John R. (Ed.), General Engineering, vol. 1. Society of Petroleum Engineers, pp. 727–765. Chap. 15.
Chu, W.C.C., Pandya, N.D., Flumerfelt, R.W., Chen, C., 2019. Rate-transient analysis based on the power-law behavior for permian wells. SPE Reservoir Eval. Eng. 22 (4), 1360–1370. https://doi.org/10.2118/187180-PA.
Clarkson, C.R., Qanbari, F., 2016. History matching and forecasting tight gas condensate and oil wells by use of an approximate semianalytical model derived from the dynamic-drainage-area concept. SPE Reservoir Eval. Eng. 19 (4), 540–552. https://doi.org/10.2118/175929-PA.
Clarkson, C.R., 2021. Unconventional Reservoir Rate-Transient Analysis. Elsevier.
Hamdi, H., Behmanesh, H., Clarkson, C.R., 2020. A semianalytical approach for analysis of wells exhibiting multiphase transient linear flow: application to field data. SPE J. 25 (6), 3265–3279. https://doi.org/10.2118/196164-PA.
Hamdi, H., Behmanesh, H., Clarkson, C.R., 2018. A semi-analytical approach for analysis of the transient linear flow regime in tight reservoirs under three-phase flow conditions. J. Nat. Gas Sci. Eng. 54, 283–296. https://doi.org/10.1016/j.jngse.2018.04.004.
Holy, R., Ozkan, E., 2017. Numerical modeling of 1D anomalous diffusion in unconventional wells using a NonUniform mesh. SPE/AAPG/SEG Unconventional Resources Technology Conference. https://doi.org/10.15530/URTEC-2017-2695593.
Li, R., Chen, Z., Wu, K., Hao, X., Xu, J., 2021. An analytical model for water-oil two-phase flow in inorganic nanopores in shale oil reservoirs. Petrol. Sci. 18 (6), 1776–1787. https://doi.org/10.1016/j.petsci.2021.09.005.
Liu, S., Li, H., Valkó, P.P., 2018. A Markov-chain-based method to characterize anomalous diffusion phenomenon in unconventional reservoir. In: SPE Canada Unconventional Resources Conference. https://doi.org/10.2118/189809-MS.
Ozcan, O., Sarak, H., Ozkan, E., Raghavan, R., 2014. A trilinear flow model for a fractured horizontal well in a fractal unconventional reservoir. In: SPE Annual Technical Conference and Exhibition. https://doi.org/10.2118/170971-MS.
Qanbari, F., Clarkson, C.R., 2013. A new method for production data analysis of tight and shale gas reservoirs during transient linear flow. J. Nat. Gas Sci. Eng. 14, 55–65. https://doi.org/10.1016/j.jngse.2013.05.005.
Qanbari, F., Clarkson, C.R., 2016. Rate-transient analysis of liquid-rich tight/shale reservoirs using the dynamic drainage area concept: examples from north American reservoirs. J. Nat. Gas Sci. Eng. 35, 224–236. https://doi.org/10.1016/j.jngse.2016.08.049.
Raghavan, R., Chen, C., 2017. Rate decline, power laws and subdiffusion in fractured rocks. SPE Reservoir Eval. Eng. 20 (3), 738–751. https://doi.org/10.2118/180223-PA.
Raghavan, R., Chen, C., 2018. A conceptual structure to evaluate wells producing fractured rocks of the Permian Basin. In: SPE Annual Technical Conference and Exhibition. https://doi.org/10.2118/191484-MS.
Shahamat, M.S., Hamdi, H., Clarkson, C.R., 2018. Analytical modeling of linear flow with variable permeability distribution in tight and shale reservoirs. J. Nat. Gas Sci. Eng. 50, 325–338. https://doi.org/10.1016/j.jngse.2017.12.020.
Shi, J.T., Wu, J.Y., Sun, Z., Xiao, Z.H., Liu, C., Sepehrnoori, K., 2020. Methods for simultaneously evaluating reserve and permeability of undersaturated coalbed methane reservoirs using production data during the dewatering stage. Petrol. Sci. 17 (4), 1067–1086. https://doi.org/10.1007/s12182-019-00410-3.
Stelson, H., 1950. Note on an extension of the method of undetermined coefficients in solving a linear differential equation. Am. Math. Mon. 57 (8), 547–549. https://doi.org/10.2307/2307942.
Stone, H.L., 1973. Estimation of three-phase relative permeability and residual oil data. J. Can. Petrol. Technol. 12 (4). https://doi.org/10.2118/73-04-06.
Valdes-Perez, A.R., Blasingame, T.A., 2020. Pressure-transient behavior of double porosity reservoirs with transient interporosity transfer with fractal matrix blocks. SPE J. 26 (4), 2417–2439. https://doi.org/10.2118/190841-PA.
Wang, W., Yuan, B., Su, Y., 2017. A composite fractal dual-porosity flow model for tight oil reservoirs with channel fractured horizontal wells. Eng. Appl. Comput. Fluid Mech. 12 (1), 104–116. https://doi.org/10.1080/19942060.2017.1348992.
Wattenbarger, R.A., El-Banbi, A.H., Villegas, M.E., Maggard, J.B., 1998. Production analysis of linear flow into fractured tight gas wells. In: SPE Rocky Mountain Regional/Low-Permeability Reservoirs Symposium. https://doi.org/10.2118/39931-MS.
Yuan, B., Su, Y., Moghanloo, R.G., Rui, Z., Wang, W., Shang, Y., 2015. A new analytical multi-linear solution for gas flow toward fractured horizontal wells with different fracture intensity. J. Nat. Gas Sci. Eng. 23, 227–238. https://doi.org/10.1016/j.jngse.2015.01.045.
Yuan, B., Moghanloo, G.R., Zheng, D., 2017. A Novel integrated workflow for evaluation, optimization and predication in shale plays. Int. J. Coal Geol. 180, 18–28. https://doi.org/10.1016/j.coal.2017.04.014.
Yuan, B., Zhang, Z., Clarkson, C.R., 2019a. Generalized analytical model of transient linear flow in heterogeneous fractured liquid-rich tight reservoirs with non-static properties. Appl. Math. Model. 76, 632–654. https://doi.org/10.1016/j.apm.2019.06.036.
Yuan, B., Zhang, Z., Clarkson, C.R., 2019b. Improved distance-of-investigation model for rate-transient analysis in a heterogeneous unconventional reservoir with nonstatic properties. SPE J. 24 (5), 2362–2377. https://doi.org/10.2118/191698-PA.
Yuan, B., Clarkson, C.R., Zhang, Z., 2021. Deviations from classical diffusion behavior: a systematic investigation of possible controls on abnormal reservoir signatures. J. Petrol. Sci. Eng. 205, 108910. https://doi.org/10.1016/j.petrol.2021.108910.
Zhang, M., Becker, M.D., Ayala, L.F., 2016. A similarity method approach for early-transient multiphase flow analysis of liquid-rich unconventional gas reservoirs. J. Nat. Gas Sci. Eng. 28, 572–586. https://doi.org/10.1016/j.jngse.2015.11.044.
Zhang, M., Vardcharragosad, P., Ayala H, L.F., 2014. The similarity theory applied to early-transient gas flow analysis in unconventional reservoirs. J. Nat. Gas Sci. Eng. 21, 659–668. https://doi.org/10.1016/j.jngse.2014.09.010.